The synthesis of diphenyl carbonate from dimethyl carbonate and phenol over mesoporous MoO$_3$/SiMCM-41

Zhenhuan Li [*], Bowen Cheng, Kunmei Su, Yu Gu, Peng Xi, Minglin Guo

College of Materials and Chemical Engineering, and Tianjin Key Lab of Fiber Modification & Functional Fiber, Tianjin Polytechnic University, Chenglin Road Number 63, Tianjin 300160, People's Republic of China

ABSTRACT

The mesoporous catalyst activities of supported molybdenum oxide for diphenyl carbonate (DPC) synthesis in liquid-phase transesterification of dimethyl carbonate (DMC) and phenol were investigated. The yields of DPC and methyl phenyl carbonate (MPC) were greatly improved when MoO$_3$ was supported on SiMCM-41 to act as catalyst. MoO$_3$/SiMCM-41 catalysts were characterized by X-ray diffraction (XRD), N$_2$ adsorption–desorption isotherms, and Fourier transform infrared (FT-IR) spectroscopy. Characterized results revealed that the high activity sites of MoO$_3$/SiMCM-41 were isolated MoO$_4{}^{2-}$ tetrahedral species and polymerized octahedral molybdenum oxide species. MPC formation increased with reaction time up to 4 h and then decreased thereafter, and maximum MPC yield achieved 39.6%. The decrease of MPC yield after 4 h might be ascribed to MPC disproportionation into DPC and reversible transesterification reaction.

Published by Elsevier B.V.

1. Introduction

DPC is used to produce many organic compounds and polymer materials, particularly as an intermediate for synthesis of polycarbonate without using phosgene [1,2]. The synthesis routes of DPC include the phosgene processes [3], carbonylation of phenol and CO$_2$ [4,5], oxidative carbonylation of phenol [6–9] and transesterification of phenol with dimethyl oxalate (DMO) [10–13] or dimethyl carbonate (DMC) [14–26]. The transesterification between DMC and phenol is considered as a better green route to synthesize DPC, because DMC is nontoxic to human health and environment [27]. This route is a two-step process, which involving the transesterification of DMC and phenol to methyl phenyl carbonate (MPC) (Eq. (1)) and the further transesterification of MPC and phenol (Eq. (2)) or disproportion of MPC to DPC (Eq. (3)) (see Scheme 1).

For transesterification of DMC and phenol to DPC, most of catalysts were acidic, for example, homogeneous catalysts such as Lewis acids [14], samarium trifluoromethanesulfonate [15], titanium esters [16] and organotin compounds [17], and heterogeneous catalysts like MoO$_3$/SiO$_2$ [18], TiO$_2$/SiO$_2$ [19–21], V$_2$O$_5$/SiO$_2$ [22]. PbO/MgO [23], lead and zinc double oxide [24], Mg–Al–hydrotalcite catalyst [25] and 12-molybdophosphoric salts [26]. In homogeneous transesterification systems, the difficult separation of

catalysts from products will cause problems. Therefore, the development of active solid catalysts is highly desirable.

Fu and Ono [18] reported that unsupported MoO$_3$ catalyst showed a very low activity because of low surface area. When molybdenum oxide was supported on SiO$_2$, ZrO$_2$, and TiO$_2$, high MPC yield was obtained. When MoO$_3$ was supported on SiO$_2$–Al$_2$O$_3$, Al$_2$O$_3$ and CaO, MPC yield was quite low but with high yields of anisole. The high yield of anisole was due to the decarboxylation of MPC into anisole when reaction was catalyzed by basic or acidic sites on supports [28–30]. Among the supports used, silica was found to be the best with respect to both the yield of and the selectivity for MPC.

The discovery of mesoporous MCM-41 materials [31,32] has given an enormous stimulus to research in heterogeneous catalysis, selective adsorption, and novel functional materials [33,34]. This is due to their outstanding advantages such as large exposed surface areas for interactions, large and defined pore sizes and enhanced surface reactivities due to their richness in reactive, coordinatively unsaturated sites, usually edges, corners, and kinks. The presence of a large number of SiOH groups on the inner surface provides the opportunity to support or anchor various functional groups by postsynthetic modification, such as chemical deposition and impregnation [35,36]. However, up to now, there were no reports on the use of mesoporous MCM-41 supported catalysts in transesterification.

Here, the effects of MoO$_3$/SiMCM-41 on DPC synthesis in liquid-phase transesterification of DMC and phenol were investigated.

---

* Corresponding author. Tel.: +86 22 24528359; fax: +86 222452 8504.
  E-mail address: zhenhuanli1975@yahoo.com.cn (Z. Li).
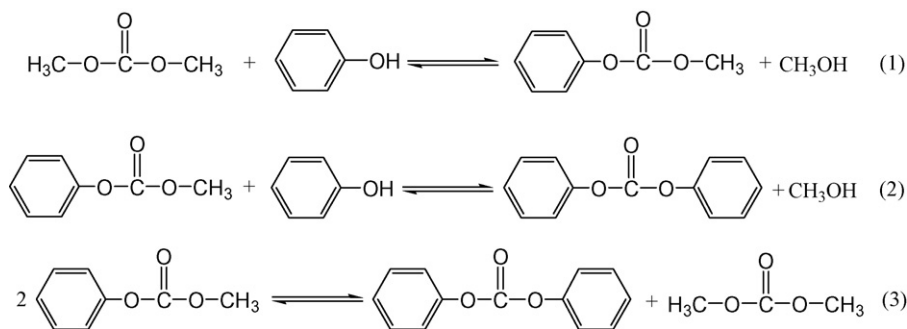
Scheme 1. DPC synthesis from transesterification of DMC and phenol.

It was found that DPC and MPC yields were greatly improved when MoO$_3$ was supported on SiMCM-41. The high activity sites on catalyst surface were the isolated tetrahedral molybdenum oxide species and polymerized octahedral molybdenum oxide species. In addition, effects of MoO$_3$ loading, time, temperature, the amount of catalyst usage and ratio of phenol to DMC on reactions were investigated.

2. Experimental

2.1. Chemical reagents

ZrOCl$_2$·8H$_2$O was purchased from Sinopharm Chemical Reagent Co., Ltd. with AR grade. (NH$_4$)$_6$Mo$_7$O$_{24}$·4H$_2$O was purchased from Tianjin Chemical Reagent Co. (IV) and used as received. Dimethyl carbonate (Tianjin Chemical Reagent Research Institute) was fractionally distilled and stored over molecular sieve (4A). Phenol (Tianjin Chemical Reagent Co. (III), China) was of analytic reagent (AR) grade and used without further purification. Other chemical reagents were analytical reagent (A.R.) grade and used as received from local manufactures without further purification.

2.2. Sample preparation

SiMCM-41 was prepared according to the documented procedure in Ref. [37]. 4.4 g hexadencyltrimethyl ammonium bromide (CTAB) and 1.1 g NaOH were dissolved in 200 mL distilled water, and the mixture was agitated to give a clear solution. 22.3 mL ethyl silicate was added into above clear solution with constant stirring to give a white precipitate gel solution which was stirred for 24 h at room temperature and heated in a sealed stainless steel autoclave at 90 °C for another 24 h. Product was recovered by filtration, washed thoroughly with distilled water and dried at 100 °C for 4 h. The removal of CTAB was carried out using alcoholic solutions of ammonium nitrate [38]. Typically, 1 g of the as-synthesized material was dispersed in 125 mL of ethanol (95%) containing 0.3 g of ammonium nitrate, and the mixture was stirred at 60 °C for 1 h. Powders were recovered by filtration and washed with ethanol and deionized water. The above treatment was repeated twice. The obtained sample was denoted as SiMCM-41.

ZrO$_2$ was prepared according to the following procedure. 4.4 g CTAB and 4.5 g NaOH were dissolved in 200 mL distilled water, and the mixture was agitated to give a clear solution. 32 g ZrOCl$_2$·8H$_2$O was dissolved in 100 mL distilled water, and then ZrOCl$_2$ solution was added drop-wise into above solution to give a white precipitate gel solution which was stirred for 24 h at room temperature and heated in a sealed stainless steel autoclave at 90 °C for another 24 h. The product was recovered by filtration, washed thoroughly with distilled water and dried at 100 °C for 4 h. The removal of CTAB was carried out using alcoholic solutions of ammonium nitrate.

γ-Al$_2$O$_3$ (BET = 161 m^2/g) was obtained from Shan Xi commodity chemistry institute, and SiO$_2$ (BET = 408 m^2/g) was purchased from Qing Dao Ocean Chemistry Corporation.

SiMCM-41, SiO$_2$, γ-Al$_2$O$_3$ and ZrO$_2$ were impregnated to incipient wetness with aqueous solutions of (NH$_4$)$_6$Mo$_7$O$_{24}$·4H$_2$O to give 10 wt% molybdenum oxide loading, and samples were dried in an oven at 110 °C for 8 h to remove moisture. At last, catalysts were activated at 500 °C for 4 h.

2.3. Characterization

N$_2$ adsorption–desorption isotherms of mesoporous samples were measured at 77 K on an ASAP2000 (Micromeritics Instrument Co., USA), prior to the measurement, all samples were outgassed at 200 °C and 10^{-6} Torr over night. The specific surface areas of mesoporous samples were calculated using the multiple-point Brunauer–Emmett–Teller (BET) method. The pore size distribution curves of samples were calculated from the adsorption branch of isotherms using the Barrett–Joyner–Halenda (BJH) method. Pore sizes were obtained from the peak positions of distribution curves.

Powder X-ray diffraction (XRD) pattern characterization of catalyst samples was measured on a Bruker AXS (Germany) diffractometer using Cu Kα radiation, and date were recorded from 10° to 45° (2θ). Fourier transform infrared (FT-IR) spectrum was obtained on a Nicolet Nexus 470 FT-IR analyzer using the KBr method.

Product structure was confirmed by GC–MS (HP5972) and compared with authentic samples. Quantitative analysis was carried on a gas chromatograph (Agilent 6890N GC with a FID detector, HP-5/DB-5 capillary column) with cetane as interior standard.

2.4. Reaction procedure

Reactions were carried out in a four-neck flask, equipped with a thermometer, nitrogen inlet, dropping funnel and fractionating column connected to a liquid dividing head. Phenol and catalyst were charged into flask under nitrogen atmosphere. When mixture was heated to 175 °C, DMC was added drop-wise, and reaction was continued for a certain period of time. During the reaction, a distillate of DMC and methanol was collected slowly in a receiver flask. After reaction finished, mixture was cooled and analyzed.

3. Results and discussion

3.1. Catalytic activities of various catalysts

The effects of supports on catalytic activities were carefully studied, and results were summarized in Table 1. The yield of DPC and MPC was 0.3 and 14.1% over 0.25 g of MoO$_3$ alone. If 0.5 g MoO$_3$ was loaded in reaction system, DPC and MPC yields were improved to 0.9 and 36.2%. When 0.5 g MoO$_3$/SiO$_2$ was employed as catalyst, the

Table 1
The catalyst activities of supported molybdenum oxides in the synthesis of diphenyl carbonate

Catalyst	Selectivity (mol%)			Yield DPC (mol%)	Yield MPC (mol%)
	Anisole	MPC	DPC		
MoO$_3$	0	99.0	1.0	0.9	36.2
MoO$_3$[a]	0	98.2	1.8	0.3	14.1
MoO$_3$/SiO$_2$	0	98.5	1.5	0.4	13.7
MoO$_3$/SiMCM-41	0	96.9	3.1	2.6	39.6
MoO$_3$/Al$_2$O$_3$	43.3	55.1	1.6	1.0	18.0
MoO$_3$/ZrO$_2$	21.2	77.3	1.5	0.3	7.9
HSiMCM-41	0	100	0	0	0.01
RMoO$_3$/SiMCM-41	0	98.7	1.3	0.21	15.6

Reaction condition: catalyst 0.5 g (MoO$_3$/SiMCM-41 with 10 wt% loading), phenol 0.2 mol, DMC 0.1 mol, reflux (175–184 °C) for 4 h.

[a] Catalyst, 0.25 g. RMoO$_3$/SiMCM-41 is the secondly used catalyst which is activated at 500 °C for 4 h.

Table 2
The physical properties of various catalysts

Catalyst	Surface area (m^2 g^{-1})	Microspore area (m^2 g^{-1})	Pore volume (cm^3 g^{-1})	Pore diameter (nm)
MoO$_3$/ZrO$_2$	141	6.0	0.33	10.0
MoO$_3$/SiO$_2$	198	–	0.44	6.0
MoO$_3$/Al$_2$O$_3$	94	–	0.31	7.1
MoO$_3$/SiMCM-41	672	–	0.80	2.7
SiMCM41	820	–	1.06	2.8

Pore diameter is maximum diameter. MoO$_3$ loading on supports is 10 wt%.

yields of DPC and MPC were 0.4 and 13.7%. While MoO$_3$/SiMCM-41 of same quantity was used as catalyst, DPC and MPC yields were greatly improved to 2.6 and 39.6%. However, Al$_2$O$_3$ and ZrO$_2$ were used as supports, an amount of anisole was detected as by-product. Among the supports used, SiMCM-41 was found to be the best with respect to the yield of DPC and MPC, and reutilization catalytic test indicated that RMoO$_3$/SiMCM-41 could be reused and showed high activity for transesterification. Nearly no reaction took place over SiMCM-41, but a little of transesterification of DMC and phenol led to high selectivity towards MPC which was difficult to further transfer into DPC without being catalyzed by high active catalyst.

In order to get a better understanding of support effects on DPC synthesis, the N$_2$ adsorption–desorption isotherms of mesoporous catalysts were measured, and characterized results were summarized in Table 2. The BET surface area of catalysts from MoO$_3$/Al$_2$O$_3$ to MoO$_3$/SiMCM-41 increased from 94 to 672 m^2 g^{-1}. The decline sequence of BET surface area (m^2 g^{-1}) was listed as following: MoO$_3$/SiMCM-41 > MoO$_3$/SiO$_2$ > MoO$_3$/ZrO$_2$ > MoO$_3$/Al$_2$O$_3$. MoO$_3$/SiMCM-41 had smaller pore diameter, but its activity was much higher than that of MoO$_3$/SiO$_2$, which might be due to the large exposed surface areas of MoO$_3$/SiMCM-41 for interactions. Although MoO$_3$/Al$_2$O$_3$ had lower BET surface, smaller pore volume and diameter, it displayed higher activity than MoO$_3$/ZrO$_2$ or MoO$_3$/SiO$_2$, which might be attributed to the high basicity of OH groups on Al$_2$O$_3$ [39] and high degree of MoO$_3$ dispersion on Al$_2$O$_3$ [40]. High anisole yield over MoO$_3$/ZrO$_2$ or MoO$_3$/Al$_2$O$_3$ was plausibly due to the decarboxylation of MPC into anisole catalyzed by basic or acidic sites on supports [18,28,29].

3.2. The effect of MoO$_3$ loading

MoO$_3$/SiMCM-41 catalysts with different molybdenum oxide loadings were prepared by the incipient wetness impregnation of SiMCM-41 supports with an aqueous (NH$_4$)$_6$Mo$_7$O$_{24}$·4H$_2$O precursor. The X-ray diffraction patterns of MoO$_3$/SiMCM-41 were

displayed in Fig. 1. MoO$_3$ crystal phase was almost undetected in 5 wt% MoO$_3$/SiMCM-41. The patterns of the catalyst containing 10 wt% MoO$_3$ provided evidence that small MoO$_3$ crystals had appeared on catalyst surface. Those characterized results were in good agreement with the literatures for alumina [41,42] and for silica systems [43]. As for MoO$_3$/SiMCM-41 catalysts with molybdenum oxide content from 20 to 30%, the XRD peaks of MoO$_3$ crystal increased markedly, which showed the presence of bulk molybdenum oxide crystal on catalyst surface.

Fig. 2 showed XRD patterns at low diffraction angles for the calcined MoO$_3$/SiMCM-41 catalysts. Three well-defined diffraction peaks indexable as (1 0 0), (1 1 0) and (2 0 0) reflections, which are associated with the hexagonal symmetry of MCM-41 type mesostructures, were observed for all these samples. The peak intensity was almost kept with an increase in molybdenum oxide
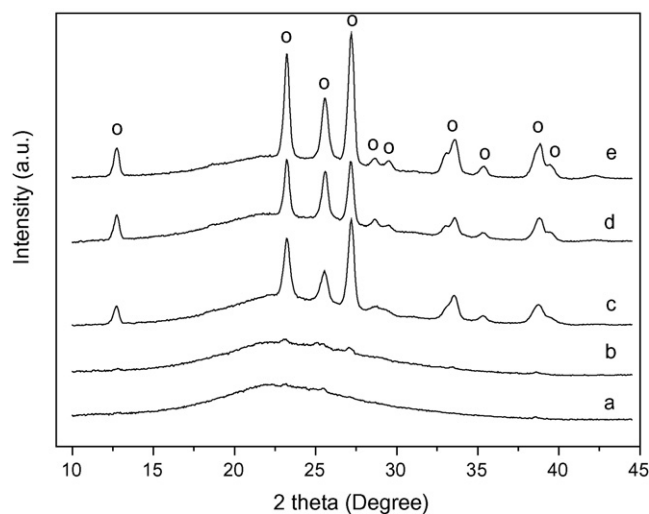

Fig. 1. XRD patterns of MoO$_3$/SiMCM-41 with different MoO$_3$ loadings: (a) 0 wt%, (b) 5 wt%, (c) 10 wt%, (d) 20 wt%, and (e) 30 wt%.
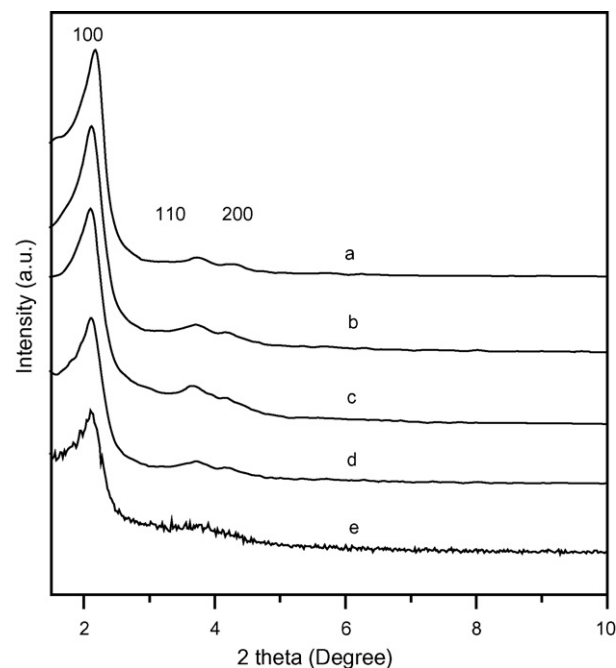

Fig. 2. Low-angle XRD patterns of MoO$_3$/SiMCM-41 catalysts with different MoO$_3$ loadings: (a) 0 wt%, (b) 5 wt%, (c) 10 wt%, (d) 20 wt%, and (e) 30 wt%.
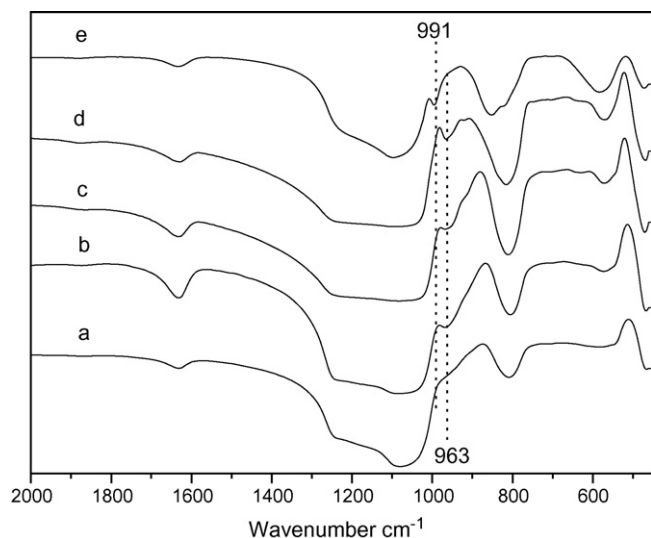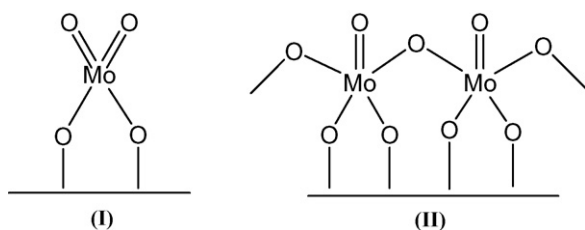
Fig. 3. FT-IR of MoO$_3$/SiMCM-41 with different MoO$_3$ loadings: (a) 0 wt%, (b) 5 wt%, (c) 10 wt%, (d) 20 wt%, and (e) 30 wt%.

Scheme 2. The isolated and polymerized molybdenum oxide species.

Fig. 4. (a) N$_2$ adsorption/desorption isotherms of MoO$_3$/SiMCM-41 and (b) BJH pore size distribution curves.

loading up to 30 wt%, suggesting that the long-range regularity of hexagonal arrays of mesopores of SiMCM-41 was sustained after the introduction of molybdenum oxide by wet impregnation technique.

FT-IR spectra were listed in Fig. 3. As for 5, 10 and 20 wt% MoO$_3$/SiMCM-41 catalysts, there was appearance of a weak broad band at 963 cm^{-1} which was characteristic of the isolated tetrahedral molybdenum species MoO$_4$$^{2-}$ (**I**) and two-dimensional polymeric form of distorted molybdenum octahedral species (**II**) [43–49] (see Scheme 2). It was worthy of noting that there were no bands detected at 963 in the spectra of 30 wt% MoO$_3$/SiMCM-41, which imply that molybdenum oxide species on the surface of 5–20 wt% MoO$_3$/SiMCM-41 catalysts were in the state of change from highly dispersed Mo species into bulk MoO$_3$, i.e., the isolated tetrahedral molybdenum species MoO$_4$$^{2-}$ and two-dimensional distorted molybdenum octahedral species transformed into three-dimensional bulk metal oxides [41,45]. Above characterized results consisted with the early report that polymeric form is growing at the expense of isolated MoO$_4$$^{2-}$ as the loading increased, and at high loadings bulk MoO$_3$ was always formed [50].

N$_2$ adsorption/desorption isotherms and pore size distribution curves of supported MoO$_3$/SiMCM-41 catalysts were displayed in Fig. 4. It was found that, for catalysts with loading from 0 to 30 wt%, N$_2$ isotherms showed well-resolved inflexions at relative pressures between 0.3 and 0.4, demonstrating that the uniform mesoporous channels in MoO$_3$/SiMCM-41 were not destroyed during catalyst preparation. However, pore size distribution measurements showed a slight decrease of average pore diameter with the increase of MoO$_3$ loading.

The effects of MoO$_3$ loading on reaction were shown in Fig. 5. The maximum DPC yield of 2.6% and MPC yield of 39.6% were obtained over catalyst with 10 wt% MoO$_3$ loading. When reaction
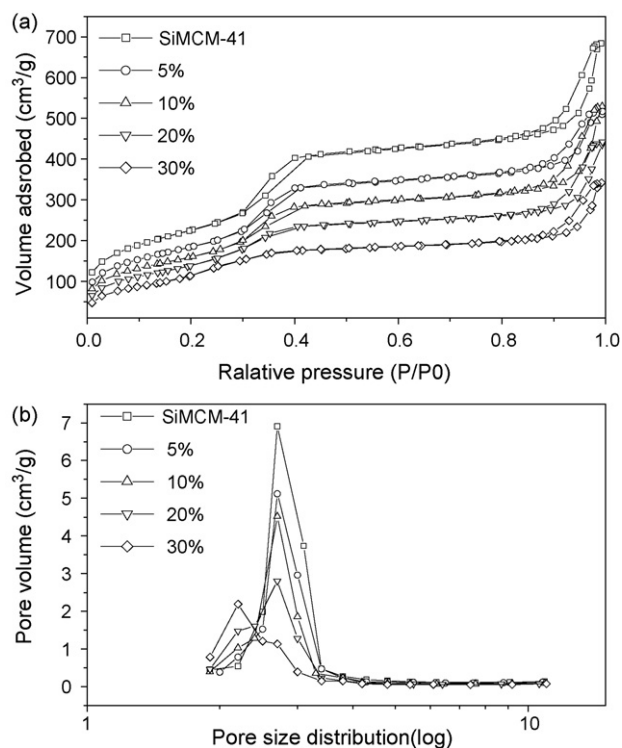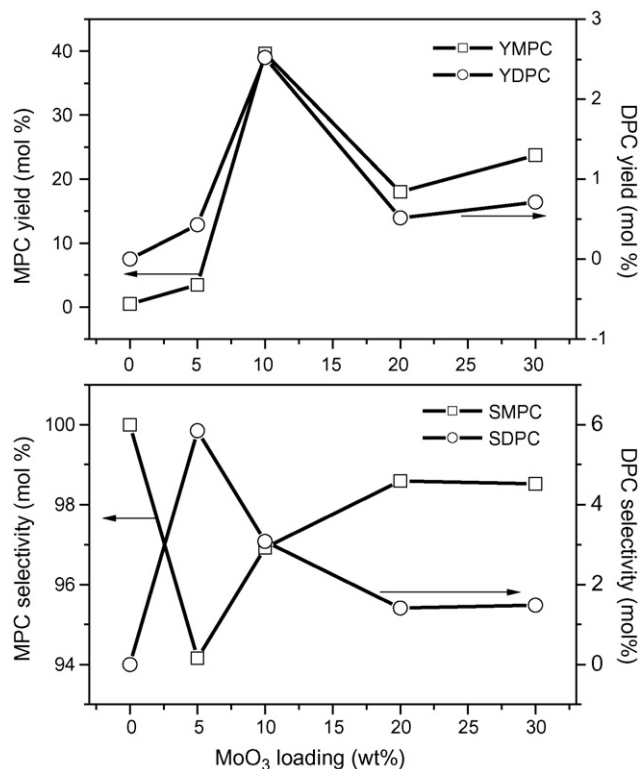

Fig. 5. Effect of MoO$_3$ loading on the MPC and DPC yield and selectivity (reaction condition: phenol 0.2 mol, DMC 0.1 mol, MoO$_3$/SiMCM-41 0.5 g, reflux 175–184 °C, 4 h).
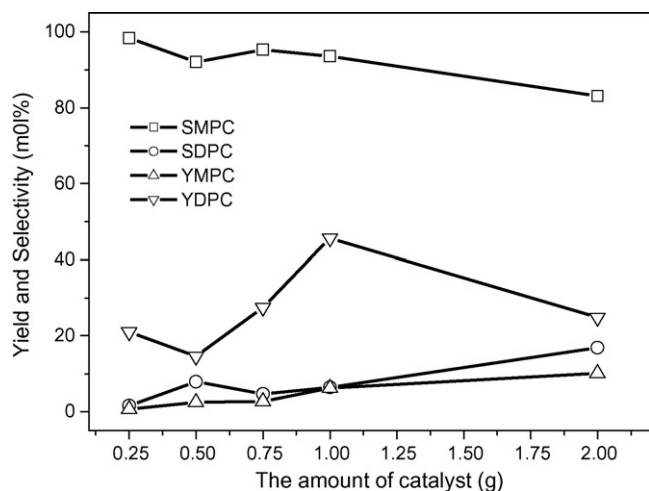
Fig. 6. Effect of 10 wt% MoO_3/SiMCM-41 amount on the transesterification of DMC and phenol (reaction condition: phenol 0.2 mol, DMC 0.1 mol, reflux 175–184 °C, 4 h).
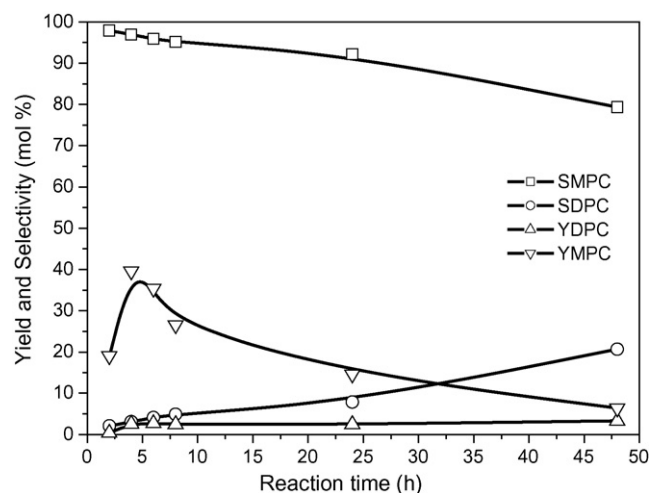

Fig. 7. Effect of reaction time on MPC and DPC selectivity and yield (reaction condition: phenol 0.2 mol, DMC 0.1 mol, reflux 175–184 °C, 10 wt% MoO_3/SiMCM-41 0.5 g).

was catalyzed by 20 wt% MoO_3/SiMCM-41, DPC and MPC yield decreased to 0.5 and 18.0%. The reason for the low activity of 20 wt% MoO_3/SiMCM-41 might be that much more isolated MoO_4^{2-} and two-dimensional molybdenum oxides on support transformed into three-dimensional bulk metal oxide species [41]. In addition, the slight decrease of average pore diameter with the increase of MoO_3 loading might be another reason for low activity of high loading catalyst which blocked the formation of MPC and DPC. However, the maximum DPC selectivity of 5.9% was observed for catalyst with 5 wt% MoO_3 loading, thereafter higher MoO_3 loading resulted in lower DPC selectivity, which suggested that highly dispersed MoO_3 on SiMCM-41 support, especially isolated MoO_4^{2-} tetrahedral species, were active sites for the transesterification of MPC and phenol into DPC.

3.3. The effect of catalyst amount on transesterification reaction

The effects of MoO_3/SiMCM-41 amount on the transesterification of DMC and phenol were studied, and results were shown in Fig. 6. When the amount of catalyst usage was 0.25 g, the yields of MPC and DPC were 21.0 and 0.7%. However, maximum MPC yield 45.7% was obtained when catalyst amount was 1 g. Thereafter, MPC yield declined from 45.7 to 28.9% with the rise of catalyst amount from 1 to 2 g, while DPC yield was improved from 6.5 to 10.1%.

3.4. The effect of reaction time

The yields of MPC and DPC were also monitored with reaction time because the transesterification of DMC and phenol was reversible, and results were listed in Fig. 7. MPC formation increased with reaction time up to 4 h and then decreased thereafter, and maximum MPC yield achieved 39.6%. DPC yield increased from 0.4 to 2.6% with reaction time increasing from 2 to 4 h. Thereafter with reaction time increasing from 4 to 48 h, a slight rise of DPC yield from 2.6 to 3.3% was observed, namely, transesterification reactions (Eq. (2)) nearly achieved equilibrium within 4 h. The decrease of MPC yield after 4 h might be ascribed to the disproportion of MPC into DPC and reversible reaction of Eq. (1).

3.5. The effect of reaction temperature

The effects of temperature on MoO_3/SiMCM-41 activity were examined, and results were listed in Fig. 8. At 160 °C and 4.0 h, the

MPC and DPC yields were 38.9 and 0.5%, respectively. When reaction was conducted at 200 °C for 4.0 h, MPC and DPC yields were 20.5 and 1.2%, respectively. Therefore, to get a better MPC yield, the favorable temperature was around 160 °C. However, high reaction temperature was in favor of DPC formation, i.e., DPC formation from MPC disproportion or transesterification of MPC and phenol often took place at high temperature.
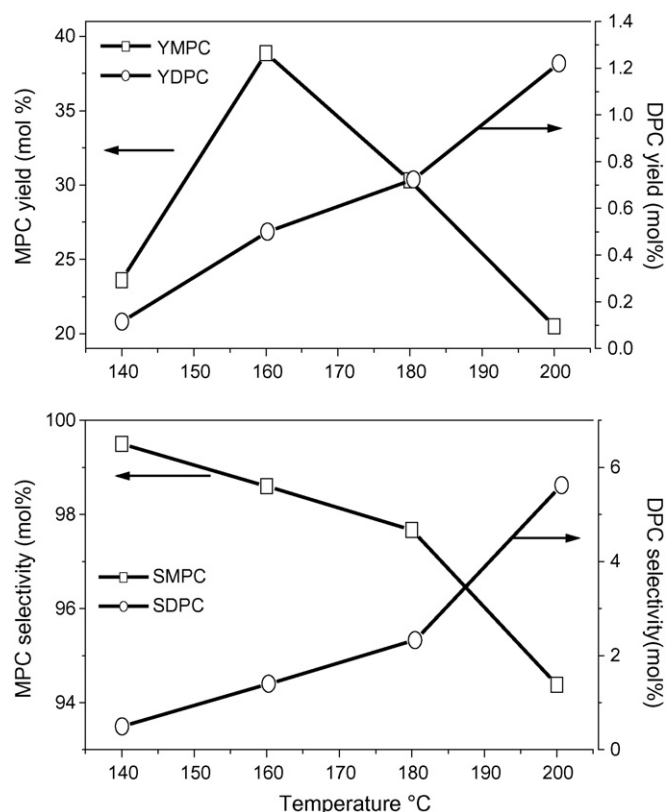

Fig. 8. Effect of reaction temperature on MPC and DPC selectivity and yield (reaction condition: phenol 0.2 mol, DMC 0.1 mol, 4 h, 10 wt% MoO_3/SiMCM-41 0.5 g).
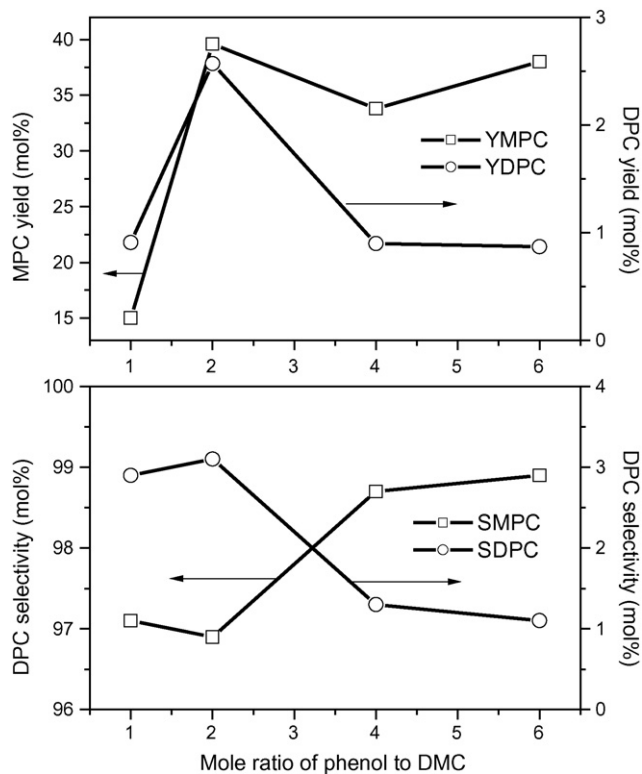
Fig. 9. Effect of phenol:DMC mole ratio on MPC and DPC selectivity and yield (reaction condition: reflux 175–184 °C, 4 h, 10 wt% MoO_3/SiMCM-41 0.5 g).

3.6. The effect of phenol/DMC mole ratio

The effects of phenol/DMC molar ratio on transesterification were investigated, and results were shown in Fig. 9. MPC yield increased from 15.0 to 38.0% as mole ratio increasing from 1 to 6 due to the availability of additional phenol for reaction. When molar ratio of phenol to DMC was below 1:1, both DPC yield and selectivity were relatively low. When phenol/DMC molar ratio increased to 2:1, DPC yield and selectivity were 2.6 and 3.1%, but thereafter both DPC yield and selectivity declined.

4. Conclusion

DPC and MPC yields were greatly improved when MoO_3 was supported on SiMCM-41. The high activity sites of MoO_3/SiMCM-41 were the isolated tetrahedral molybdenum oxide species and the polymerized octahedral molybdenum oxide species. The highly dispersed MoO_3 on SiMCM-41 support, especially the isolated MoO_4^{2-} tetrahedral species, were active sites for transesterification of MPC and phenol into DPC.

MPC formation increased with reaction time up to 4 h and then decreased thereafter, and maximum MPC yield achieved 39.6%. The decrease of MPC yield after 4 h might be ascribed to the disproportion of MPC to DPC and reversible reaction of Eq. (1). To get a better MPC yield, the favorable temperature was around 160 °C, however, high reaction temperature was in favor of DPC formation. MPC yield

went up as the mole ratio of phenol to DMC increasing from 1 to 6 due to the availability of additional phenol for reaction, while the molar ratio of phenol/DMC increased to 2/1, the yield and selectivity of DPC were 2.6 and 3.1%, but thereafter both DPC yield and selectivity declined.

References

[1] S.P. Kim, J.S. Lee, S.H. Kim, B.H. Lee, S.H. Kim, J. Ind. Eng. Chem. 5 (1999) 268.
[2] W.B. Kim, U.A. Joshi, J.S. Lee, Ind. Eng. Chem. Res. 43 (2004) 1897.
[3] J. Gong, X. Ma, S. Wang, Appl. Catal. A 316 (2007) 1.
[4] Z. Li, Z. Qin, H. Zhu, J. Wang, Chem. Lett. 35 (2006) 784.
[5] Z. Li, Z. Qin, J. Mol. Catal. A 264 (2006) 255.
[6] M. Goyal, R. Nagahata, J. Sugiyama, M. Asai, M. Ueda, K. Takeuchi, J. Mol. Catal. A 137 (1999) 147.
[7] H. Ishii, M. Goyal, M. Ueda, K. Takeuchi, M. Asai, Catal. Lett. 65 (2000) 57.
[8] H. Ishii, M. Goyal, M. Ueda, K. Takeuchi, M. Asai, J. Mol. Catal. A 148 (1999) 289.
[9] H. Ishii, M. Ueda, K. Takeuchi, M. Asai, J. Mol. Catal. A 144 (1999) 369.
[10] J. Gong, X. Ma, X. Yang, S. Wang, N. Gao, D. Wang, Catal. Lett. 99 (2005) 187.
[11] J. Gong, X. Ma, X. Yang, S. Wang, S. Wen, Catal. Commun. 5 (2004) 179.
[12] J. Gong, X. Ma, S. Wang, M. Liu, X. Yang, G. Xu, J. Mol. Catal. A 207 (2004) 215.
[13] X. Ma, J. Gong, X. Yang, S. Wang, Appl. Catal. A 280 (2005) 215.
[14] H. Yasuda, K. Watarai, J.C. Choi, T. Sakakura, J. Mol. Catal. A 236 (2005) 149.
[15] F.M. Mei, G.X. Li, N. Jin, H.B. Xu, J. Mol. Catal. A 184 (2002) 465.
[16] H. Niu, J. Yao, Y. Wang, G. Wang, Catal. Commun. 8 (2007) 355.
[17] Z. Du, W. Kang, T. Cheng, J. Yao, G. Wang, J. Mol. Catal. A 246 (2006) 200.
[18] Z.H. Fu, Y. Ono, J. Mol. Catal. A 118 (1997) 293.
[19] W.B. Kim, J.S. Lee, J. Catal. 185 (1999) 307.
[20] W.B. Kim, J.S. Lee, Catal. Lett. 59 (1999) 83.
[21] W.B. Kim, Y.G. Kim, J.S. Lee, Appl. Catal. A 194/195 (2000) 403.
[22] Z. Li, Z. Qin, J. Wang, Shiyou Huagong 35 (2006) 528 (in Chinese).
[23] M. Cao, Y. Meng, Y. Lu, Catal. Commun. 6 (2005) 802.
[24] W.Q. Zhou, X.Q. Zhao, Y.J. Wang, J.Y. Zhang, Appl. Catal. A 260 (2004) 19.
[25] F.M. Mei, Z. Pei, G.X. Li, Org. Process. Res. Dev. 8 (2004) 372.
[26] T. Chen, H. Han, J. Yao, G. Wang, Catal. Commun. 8 (2007) 1361.
[27] A. Vavasori, L. Toniolo, J. Mol. Catal. A 151 (2000) 37.
[28] P. Braunstein, M. Lakkis, D. Matt, S. Lecolier, J. Mol. Catal. A 42 (1987) 353.
[29] G. Barcelo, D. Grenouillat, J.P. Senet, G. Sennyey, Tetrahedron 46 (1990) 1839.
[30] Y. Ono, Appl. Catal. A 155 (1997) 133.
[31] C.T. Kresge, M.E. Leonowicz, W.J. Roth, J.C. Vartuli, J.S. Beck, Nature 359 (1992) 710.
[32] J.S. Beck, J.C. Vartuli, W.J. Roth, M.E. Leonowicz, C.T. Kresge, K.D. Schmitt, C.T.W. Chu, D.H. Olson, E.W. Sheppard, S.B. Mccullen, J.B. Higgins, J.L. Schlenker, J. Am. Chem. Soc. 114 (1992) 10834.
[33] A. Corma, Top. Catal. 4 (1997) 249.
[34] A. Stein, B.J. Melde, R.C. Schroden, Adv. Mater. 12 (2002) 1403.
[35] R. Anwander, Chem. Mater. 13 (2001) 4419.
[36] R. Anwander, I. Nagl, M. Widenmeyer, C. Engelhardt, O. Groeger, C. Palm, T. Roser, J. Phys. Chem. B 104 (2000) 3532.
[37] M.H. Lim, A. Stein, Chem. Mater. 11 (1999) 3285.
[38] Q. Tang, Y. Xu, D. Wu, Y. Sun, J. Wang, J. Xu, F. Deng, J. Control. Release 114 (2006) 41.
[39] A.N. Desikan, L. Huang, S.T. Oyama, J. Chem. Soc., Faraday Trans. 88 (1992) 3357.
[40] S. Braun, G.A. Lucia, V.L. Camorim, M. Schmal, J. Phys. Chem. B 104 (2000) 6584.
[41] Y.C. Xie, Y.Q. Tang, Adv. Catal. 37 (1990) 1.
[42] B. Mahipal Reddy, E. Padmanabha Reddy, S.T. Srinivas, J. Catal. 136 (1992) 50.
[43] S.R. Stampfl, Y. Chen, J.A. Dumesic, C. Niu, C.G. Hill Jr., J. Catal. 105 (1987) 445.
[44] C. Li, J. Catal. 216 (2003) 203.
[45] J. Leyrer, R. Margraf, E. Taglauer, H. Knözinger, Surf. Sci. 201 (1988) 603.
[46] J. Leyrer, D. Mey, H. Knözinger, J. Catal. 124 (1990) 349.
[47] R. Margraf, J. Leyrer, E. Taglauer, H. Knozinger, Surf. Sci. 189/190 (1987) 842.
[48] G. Mestl, T.K.K. Srinivasan, Catal. Rev. Sci. Eng. 40 (1998) 451.
[49] H. Jeziorowski, H. Knoezinger, J. Phys. Chem. 83 (1979) 1166.
[50] J. Medema, C. van Stam, V.H.J. de Beer, A.J.A. Konings, D.C. Koningsberger, J. Catal. 53 (1978) 386.